Interactions between Barrier Islands and Backbarrier Marshes Affect Island System Response to Sea Level Rise: Insights from a Coupled Model

David Walters[1,2], Laura J. Moore[1], Orencio Duran[1,3], Sergio Fagherazzi[4], and Giulio Mariotti[4,5]

[1]Department of Geological Sciences, University of North Carolina at Chapel Hill, Chapel Hill, NC, United States.

[2]Now at Department of Physical Sciences, Virginia Institute of Marine Science, Gloucester Point, VA, United States.

[3]Now at MARUM-Center for Marine Environmental Sciences, University of Bremen, Bremen, Germany.

[4]Earth Science and Center for Computational Science, Boston University, Boston, MA, United States.

[5]Now at Earth, Atmospheric and Planetary Sciences, Massachusetts Institute of Technology, Cambridge, MA, United States.

Correspondence to: David Walters, dcwalters@vims.edu

Abstract

Interactions between backbarrier marshes and barrier islands will likely play an important role in determining how low-lying coastal systems respond to sea level rise and changes in storminess in the future. To assess the role of couplings between marshes and barrier islands under changing conditions, we develop and apply a coupled barrier island-marsh model (*GEOMBEST+*) to assess the impact of overwash deposition on backbarrier marsh morphology and of marsh morphology on rates of island migration. Our model results suggest that backbarrier marsh width is in a constant state of change until either the backbarrier basin

becomes completely filled or backbarrier marsh deposits have completely eroded away. Results also suggest that overwash deposition is an important source of sediment, which allows existing narrow marshes to be maintained in a long-lasting alternate state (~500 m wide in the Virginia Barrier Islands) within a range of conditions under which they would otherwise disappear. The existence of a narrow marsh state is supported by observations of backbarrier marshes along the eastern shore of Virginia. Additional results suggest that marshes reduce accommodation in the backbarrier bay, which, in turn, decreases island migration rate. As climate change results in sea level rise, and the increased potential for intense hurricanes resulting in overwash, it is likely that these couplings will become increasingly important in determining future system behavior.

1. Introduction

1.1 Background

Barrier islands are narrow, low-lying landforms that are separated from the mainland by shallow (often marsh-filled) bays. These coastal landforms are popular landforms on which to live or vacation and yet they are highly dynamic and vulnerable to changing environmental conditions. In addition to the economic importance of barrier islands themselves [*Zhang and Leatherman*, 2011], the low-energy basins sheltered by islands are also valuable commodities, as indicated by economic assessment of marsh ecosystem services [*Costanza et al.*, 1997]. As climate change leads to accelerated relative sea level rise (RSLR) [e.g., *IPCC*, 2014; *Vermeer and Rahmstorf*, 2009] and the potential for more frequent or intense major hurricanes [e.g., *Bender et al.*, 2010; *Knutson et al.*, 2010; *Emanuel*, 2013], barrier islands and their associated marshes and shallow bays will respond by migrating landward. Overwash (the transport of sand from the front toward the back of a barrier) facilitates this landward migration, allowing sandy islands to roll over backbarrier marshes (i.e., those marshes that are located along the landward

shoreline of barrier islands), as they increase in elevation both through overwash deposition and by moving to higher ground. Backbarrier marshes in turn prograde into backbarrier bays in response to sea level rise, and bays flood the mainland.

As sea level rises, barrier island migration tends to occur at a rate sufficient to liberate enough sand from the shoreface to provide the rate of overwash deposition necessary for the island to maintain its position relative to sea level [e.g., *Hoyt*, 1967; *Swift*, 1975; *Bruun*, 1988; *Zhang et al.*, 2004; *Masetti et al.*, 2008; Moore et al., 2010]. Factors that control rates of island migration include: RSLR rate, underlying geology, [e.g., *Riggs et al.*, 1995], influence of stratigraphy [e.g., *Belknap and Kraft*, 1985; *Storms et al.*, 2002; *Moore et al.*, 2010;], sediment grain size [e.g., *Storms et al.*, 2002; *Masetti et al.*, 2008], substrate slope [*Storms et al.*, 2002; *Wolinsky and Murray*, 2009; *Moore et al.*, 2010] and substrate erodibility [*Moore et al.*, 2010]. Among these, recent work suggests that substrate sand content (affecting rate of sand supply to the island) and RSLR rate are most important [*Moore et al.*, 2010]. Recent modeling experiments, conducted using the morphological behavior model, GEOMBEST (Geomorphic Model of Barrier, Bay and Shoreface Translations), also suggested that barrier islands are sensitive to changes in the substrate slope and sand content of the backbarrier region such that an increase in either one leads to a decrease in landward migration rates. This indicates that backbarrier sedimentation can play an important role in maintaining steady rates of island migration into the future [*Brenner*, 2012].

As sea level rises, tidal salt marshes aggrade via the vertical accretion of fine-grained sediment (largely due to frequent flooding by sediment-laden water) thereby maintaining elevation of the marsh platform relative to sea level and keeping marsh plants within the elevation range to which they are adapted [*French*, 1993]. The rate at which a marsh accretes is

dependent on fine-grained sediment input [e.g., *Kirwan et al.*, 2011; *Mudd*, 2011; *Gunnell et al.*, 2013] and bio-physical feedbacks such as an increase in the growth rate and subsequent organic deposition of the salt marsh macrophyte *Spartina alterniflora* in response to an increase in the depth below high tide [*Cahoon and Reed*, 1995; *Morris et al.*, 2002; *Mudd et al.*, 2010; *Kirwan et al.*, 2011]. Due to these feedbacks, marsh platforms are stable (i.e., able to maintain elevation relative to sea level) under a range of conditions, but at high RSLR rates and low fine-grained sediment supply rates, marshes can transition to become tidal flats, which is an alternative stable state [*Fagherazzi et al.*, 2006; *Mariotti et al.*, 2010]. Using a hydrodynamic model of sediment transport and wave-based erosion at the bifurcation between tidal flats and salt marshes, *Mariotti and Fagherazzi* [2010] suggested that the transition boundary between the two is never in equilibrium. Instead, the boundary is always either prograding into the tidal flat and creating new marsh or eroding into the marsh platform and creating more tidal flat, as a function of the fine-grained sediment supply to the marsh relative to the RSLR rate.

Although our understanding of how barrier islands and marshes respond to climate change continues to improve, we know little about how the connectivity of these two landscape systems (e.g., via overwash deposition, accommodation) affects the evolution of coupled barrier-marsh systems under changing conditions. For example, under rising sea level, a backbarrier marsh will lose areal extent equal to the rate at which the barrier island rolls over the marsh platform, unless the marsh progrades into the bay or up the mainland slope as it is flooded by the rising sea level. Meanwhile, contributions to marsh accretion via overwash deposition may enhance the ability of a marsh to keep up with RSLR in which case less fine-grained sediment will be needed to maintain marsh elevation. The coupling may operate in the other direction in that the presence of a marsh platform reduces accommodation space (i.e., the volume of empty space behind the

94 island that would need to be filled with sediment in order to reach sea level, hereafter referred to
95 as accommodation) as an island migrates across the backbarrier region in response to RSLR.
96 Since a reduction in accommodation decreases the amount of sand needed to maintain island
97 elevation relative to sea level, this has the potential to reduce the rate at which the island needs to
98 migrate, assuming conservation of barrier sand. In addition, the composition (i.e., sand
99 percentage) and erodibility of the substrate encountered by an island will be partially determined
100 by the character of the sediments that have been deposited in the backbarrier environment
101 [*Brenner*, 2012]. Cross-shore variations in sediment composition and erodibility can also impact
102 the rate of island migration.
103 To quantify the feedbacks between barrier islands and fringing backbarrier marshes we
104 couple the morphological-behavior model for island migration, GEOMBEST [*Stolper et al.*,
105 2005; *Moore et al.*, 2010], to the marsh-tidal flat model presented in *Mariotti and Fagherazzi*
106 [2010]. Using *GEOMBEST+* we run two sets of model experiments to test the impact of islands
107 on marshes and vice versa. In the first set of experiments, we assess the impact of barrier island
108 processes on marsh morphology by investigating how changes in overwash deposition and RSLR
109 affect marsh progradation and marsh width. We then use observations from satellite imagery to
110 provide support for the findings resulting from these experiments. In the second set of
111 experiments, we assess the impact of backbarrier morphology and sedimentary characteristics on
112 long-term rates of island migration by investigating how long-term barrier island landward
113 migration is affected by differences in backbarrier marsh width and sand content.
114

2. Methods: Modeling a Coupled Barrier Island-Marsh System

2.1 Study Area – The Virginia Barrier Islands and Metompkin Island

The Virginia Barrier Islands (VBIs) — a landwardly-migrating barrier island chain located on the Delmarva Peninsula on the U.S. mid-Atlantic coast — includes the Virginia Coast Reserve which is owned and managed by The Nature Conservancy and is also a Long Term Ecological Research site (Figure 1A). There has been little direct human impact on the islands and backbarrier environments of the VBIs, which makes them an ideal natural laboratory in which to study barrier island and salt marsh processes. The VBIs are located within a hot spot of RSLR where RSLR rate increases over the past 60 years are 3-4 times the global average [*Sallenger et al.*, 2012] and have been experiencing an average RSLR rate of 3-4 mm/yr over that time period [*Porter et al.*, 2013].

We use Metompkin Island and the associated fringing backbarrier marsh, located in the VBIs (Figure 1A), to develop generalized model inputs for use in simulations designed to provide insights into the evolution of coupled barrier-marsh systems in general. Metompkin Island is 10-km long, 100 m – 500 m wide (average ~ 250 m), and is frequently overwashed, especially along its southern half. The southern half of Metompkin Island is backed by a shallow bay, while an extensive marsh platform mostly fills the backbarrier basin along the northern half of the island (Figure 1B).

2.2 Model Description: Developing GEOMBEST+

We develop a new model to study couplings between barrier islands and backbarrier marshes by coupling GEOMBEST [*Stolper et al.*, 2005; *Moore et al.*, 2010] to a model of the migration of the marsh-tidal flat boundary [*Mariotti and Fagherazzi* 2010]. In its original form, GEOMBEST is a two-dimensional (elevation and cross-shore distance) morphological behavior

model that simulates barrier island evolution in response to changes in sea level and sand supply. GEOMBEST simulates the morphologic and stratigraphic evolution of shoreface, barrier and bay environments over the time scale of decades to millennia. We provide a brief description of model formulation and inputs here. For a more detailed discussion of the model, we refer the reader to *Stolper et al.* [2005] and *Moore et al.* [2010].

GEOMBEST is formulated under sand conservation principles, meaning that it accounts for (and balances) sand sources and sinks; fine-grained sediments, on the other hand, are lost from the system when eroded. Sources of sand include shoreface erosion and/or alongshore sand transport (AST) (where gradients in AST are positive). In contrast, sand deposited on the subaerial island and in the backbarrier, as well as sand lost to AST (where gradients are negative), represent sinks. The model is also formulated under the assumption that, over long time scales, a barrier island and shoreface profile will tend to remain invariant, such that an equilibrium profile shape (i.e., morphology) tends to be maintained. Morphological evolution is driven in the model by differences between an equilibrium profile that extends from the shoreface to the backbarrier marsh and the existing island morphology, defined in a 2-dimensional grid of surface morphology and stratigraphy. After each time step the equilibrium profile is shifted upward to maintain its position relative to sea level, and shifted horizontally to a position that best conserves sand. However, in some cases, the simulated profile may depart from the specified equilibrium morphology, for example, if the depth-dependent erosion and accretion rates are not sufficient for the equilibrium morphology to be maintained by shoreface erosion [Moore et al., 2010] (although this case does not apply in the simulation experiments reported on here).

Three functional domains are defined in GEOMBEST: shoreface, barrier island, and backbarrier bay (Figure 2A). The shoreface is defined as the ocean-side portion of the barrier island that is below mean sea level and extends to the base of the shoreface (i.e., the shoreface depth), where the effect of wave energy on sediment transport is negligible. Within the model, the barrier island is defined as the subaerial portion of the island from the shoreline to the first point at sea level on the bayward side of the island, thus including the backbarrier marsh platform. The backbarrier bay is the region below sea level that extends from the barrier island to the mainland. The user-defined equilibrium morphology includes the shoreface and barrier island domains, while the backbarrier bay evolves according to a fixed rate of sedimentation. A principal feature of GEOMBEST is the ability to define distinct stratigraphic units that describe the sedimentary characteristics (i.e., sand content and erodibility) of each unit. The erodibility and sand content parameters are important because they constrain the volume of sand that can be liberated by erosion of the shoreface in a given time step, and thus directly affect island migration (e.g., substrates with a higher sand content reduce the rate of island migration necessary to liberate sufficient sand to maintain island elevation above sea level, relative to substrates containing less sand).

The new model we have developed—which we call *GEOMBEST+*—differs from previous versions of GEOMBEST in several ways. (Note: Since we conducted all simulations using only *GEOMBEST+*, hereafter, we discuss only this new version of the model.) Perhaps most importantly, in *GEOMBEST+*, the equilibrium morphology that tends to be maintained under most conditions does not extend to the backbarrier marsh. Rather, past the topographic low located at the high tide line on the landward side of the island (referred to here as the dune limit), the backbarrier evolves dynamically such that the marsh either progrades into the bay or erodes

as a function of the rate of sea level rise and the availability of fine-grained sediment, as in *Mariotti and Fagherazzi* [2010]. We altered the functional realms in *GEOMBEST+* such that the marsh is now considered part of the backbarrier realm, which is filled with a combination of bay and marsh (Figure 2B). *GEOMBEST+* also includes a new stratigraphic unit representing the marsh, and a new index parameter to describe the stratigraphic layers (in addition to sand content and erodibility), known as the organic content, which gives the volume fraction of the sedimentary bed that is occupied by organic matter rather than mineral sediment. This allows *GEOMBEST+* to include the contribution of internally supplied organic sediments to the barrier system, which was not represented in the previous iteration of the model. We ran all simulations using a cell size of 50 m in width by 0.1 m in height, and time steps of 10 years, although the backbarrier processes iterate on a shorter time scale (over a sub-time step in the model), calculated within the model as the time it takes for the bay to reach an equilibrium depth at which the rates of erosion and accretion are equal (backbarrier depth typically reached equilibrium in 3-5 years in the model).

In *GEOMBEST+*, the backbarrier basin is comprised of a combination of marsh and bay ranging from completely filled with marsh to completely empty. Marsh growth is limited by the fine-grained sediment supply, and cannot exceed the accommodation afforded by rising sea level. When there is sufficient sediment available, the marsh unit grows at the mainland and backbarrier boundaries of the bay in the intertidal zone (between the high water line and mean sea level), with an internal input of organic sediment and an external flux of fine-grained sediments exported from the bay. Overwash provides a potential additional supply of sediment for the backbarrier. Aeolian transport is another potential source of sand to the backbarrier, but it

decreases to a negligible amount at a distance of >20m from the dune limit [*Rodriguez et al.*, 2013], and is therefore not included in this formulation of *GEOMBEST+*.

In the model, overwash occurs via removal of sand from the budget of the shoreface/island and addition of the same amount of sand into the backbarrier. The model simulates the effect of multiple overwash events over time, rather than individual storms, thus the removal of sand from the barrier does not follow any pattern of shoreface erosion and recovery, and the overwash is emplaced in a single continuous layer over the marsh/bay. This sand is then preserved in the stratigraphy of the backbarrier, conserving sand within the system by transferring it from the barrier to the marsh/bay. Two parameters control overwash deposition in *GEOMBEST+*: the overwash volume flux (Q_{OW}) and the maximum overwash accretion rate (A_{OW0}). These parameters determine the morphology of the overwash fan across the backbarrier region for a given time step. Deposition starts at the dune limit with a rate A_{OW0}, which is prescribed as an input parameter, and extends landward, with the rate of sediment deposition decaying exponentially according to:

$$A_{OW}(x) = A_{OW_0} * \exp^{-x/L_{OW}} \quad (1)$$

$$L_{OW} = \frac{Q_{OW}}{A_{OW_0}} \quad (2)$$

where A_{OW} is the overwash accretion rate at a distance x from the dune limit and L_{OW} is the typical length scale over which the overwash deposit extends into the backbarrier. For a given overwash sand supply into the backbarrier Q_{OW}, a greater accretion rate A_{OW0} will result in a thicker and less areally-extended overwash fan. Conversely, a small A_{OW0} implies a thinner and more aerially-extensive overwash fan. Consistent with the overall formation of GEOMBEST, we vary these parameters within *GEOMBEST+* to create overwash deposits representing a range of

cumulative storm effects over time rather than directly representing storm activity/intensity and simulating the deposition of individual storm overwash layers.

The bay sediment flux (Q_B) represents the volume flux of fine-grained sediment supply across the bay from a combination of fluvial inputs, temporary storm-surge channels, and inlet exchange [*Boothroyd et al.*, 1985]., Q_B sets the budget for the net import of sediment to the bay, not including sediment from overwash. It can be positive or negative to reflect a net import or export of sediment to and from the backbarrier bay. In the model, the bay accretion rate A_B is determined from Q_B:

$$A_B = \frac{Q_B}{L_B} \tag{3}$$

where L_B is the cross-shore dimension of the backbarrier bay. The accretion rate is constant everywhere in the bay, as it is assumed that sediments are redistributed across- and along-shore. The depth dependent erosion rate (E) is determined as:

$$E(x) = E_{\max}\left(\frac{1-d(x)}{d_R}\right) \tag{4}$$

where E_{max} is the maximum erosion rate for the bay, a parameter determined by the potential for the development of high-energy waves in the backbarrier basin (related to wind climate and fetch), d is the depth of the bay below mean sea level at position x, and d_R is the depth below mean sea level below which wave energy does not cause net erosion. The evolution of the bay depth at a given position x then results from the balance between overwash accretion, bay accretion and erosion and the RSLR rate, R(R):

$$\frac{\partial d}{\partial t} = R + E(x) - A_B - A_{OW}(x)\,. \tag{5}$$

The sediment that is resuspended due to bay erosion is then deposited at the outer boundaries of the bay, following the work of *Mariotti and Fagherazzi* [2010], which shows that sediments are preferentially accumulated at the landward and barrier island boundaries of a tidal flat. Once the cell at the bay boundary accretes to the low tide line (d_L), vegetative growth augments the accretion rate through the deposition of organic matter, which we assume to be a constant fraction of the marsh sediments, O_C:

$$\frac{A_M}{2} = \begin{cases} E & d > d_L \\ E + E * O_c & d < d_L \end{cases} \quad (6)$$

where A_M, the accretion rate of the cell at the bay boundary, is divided by two, since there is a boundary cell on either end of the two-dimensional bay (Figure 2; Table 1). The marsh accretes vertically up to the high water level (*HWL*), and then accretion begins in the next bayward cell, leading to marsh progradation (*P*), following the formulation:

$$P = A_M / (HWL - d(x)) * dx \quad (7)$$

where *dx* is the width of the cell in the model. This progradation occurs equally at both boundaries of the marsh. When fine-grained sediment supply is insufficient for the marsh edge to prograde, the marsh boundary remains stationary. The model does not simulate erosion of the edge of the marsh platform by waves, but the model will erode and resuspend sediment if the platform falls below sea level.

2.3 Model Inputs for Marsh-Width Experiments

We use the newly formulated *GEOMBEST+* in this set of experiments to better understand how backbarrier marshes are affected by the input of sandy sediment from an adjacent barrier island (via overwash deposition) relative to the input of tidally-delivered fine-grained sediment from an adjacent bay, as sea level rises. To assess the relative effect of the two sources of

sediment, we run a set of experiments for which we systematically vary (from one simulation to the next) R, Q_B, and Q_{OW} one at a time (within the range of values reported in Section 2.3 and Table 1). (Note: We also co-vary A_{OW} with Q_{OW}, to maintain overwash deposition at a constant width.) Varying parameter values in this way across 3 different initial conditions results in 3,000 individual simulations.

2.3.1 Initial Morphology and Stratigraphy

For the experiments to study the impact of barrier and backbarrier processes on marsh width, we derived a simplified initial condition for our experiments from a stratigraphy and morphology which was developed by *Brenner* [2012] from 5 cross-shore profiles extracted from LIDAR (NASA: Charts 2005), and bathymetric data (NOAA National Coastal Elevation Model) along multiple transects spaced at 1-km intervals across the southern half of Metompkin Island. To simplify, we smoothed the average profile developed by *Brenner* [2012] and combined the underlying stratigraphic units (a sandier late-Pleistocene fluvial deposit and a muddier early-Holocene lagoonal unit) into one generic underlying facies by averaging the estimated sand content and erodibility of the two. This idealized morphology and stratigraphy fits well with the goal of our study, which is to assess the role of couplings between marshes and barrier islands, rather than to make any predictions about the behavior of a specific barrier island and the effects of its specific stratigraphy.

To constrain sand content for the backbarrier marsh stratigraphic unit, we analyzed 9 cores collected from 6 sites along cross-shore and alongshore transects, parallel and perpendicular to a small overwash fan on Metompkin Island (Figure 1C) with the goal of determining how sediment characteristics vary with depth and location. Cores extended to a

depth of 200 cm unless a non-peat layer was reached at a shallower depth. We sampled 1 cm segments from the core at 5 cm intervals, and dried the sediment samples overnight at 60° C, to determine the dry weight of each sample. We subsampled the 1 cm sections of core in replicate, analyzed for sand content using a Beckman Coulter Laser Particle Size Analyzer LS 13 320, and used the resultant grain size distribution to determine sand percent (by volume) within the cores.

The overall trend across sampling locations indicates that sand percent is greatest near the dune limit (sample sites C, D, E, and F; with average sand percent of 43, 90, 12 and 54, respectively) and decreases exponentially to the marsh edge (sample sites A and B; with sand percent of 18 and 20, respectively) (Figure 3), suggesting (as expected) that aeolian and/or overwash deposition decreases with distance landward from the dune limit. Results from cores A and B—from the interior of the marsh platform—suggest a transition from a low-organic-content/high-sand-content bay environment to a high-organic-content/low-sand-content marsh environment at a depth of ~46-32 cm (Figure 3A & B). Within the identified marsh unit (0- ~32 cm) of cores A and B the average sand percentage is 9.5 and 10.8, respectively, which we use as the basis for setting the sand content for the marsh unit to 10% (index value = 0.1), for all experiments (Table 1).

Initial conditions are the same for all simulations except that we run replicate experiments in which we vary the initial proportion of open bay and salt marsh in the backbarrier basin. Here we consider an 1800 m-wide open bay without marsh (i.e., empty basin), a 1000 m-wide bay fringed by a 400 m-wide (i.e., narrow marsh) marsh on both the barrier island and mainland side, and a basin completely filled by an 1800 m-wide marsh (i.e. filled basin). These initial conditions are representative of the backbarrier marsh widths shown to be most prevalent on Metompkin Island (see section 3.1.2).

318 *2.3.2 Organic Content of Marsh Stratigraphic Unit*

319 To develop an estimate for volumetric organic content (O_C) in the marsh, we measured
320 organic mass content in our cores via loss on ignition (LOI), following the methods of *Chmura*
321 *and Hung* [2004]. The LOI measurements from the previously-identified marsh units in cores A
322 and B (Section 2.3.1) indicate that the backbarrier marsh on Metompkin Island contains ~9.3%
323 organic matter by mass, on average, which compares well with studies of marshes of similar ages
324 in other parts of the VBIs [*Osgood and Zieman,* 1993]. To derive O_C, we must convert from the
325 percent organic matter by mass to yield a volume percent. According to *Weinstein and Kreeger*
326 [2000] a given increase in the mass of organic matter results in an increase in accretion rate that
327 is approximately 10 times greater than for the same increase in the mass of mineral matter, which
328 suggests that organic matter is responsible for filling ~10 times more volume than mineral
329 matter. Based on this, we assume that the mineral sediment has a bulk density of ten times the
330 organic sediment (neglecting the porosity differences between the two) which yields an organic
331 content fraction for the marsh of 0.5 (Table 1).
332
333 *2.3.3 Parameterization of Overwash*

334 We vary overwash volume flux (Q_{OW}) from 0 to 2 m^3/m/yr per 1 m in the alongshore
335 direction (Table 1). This falls within the range of values reported from surveys of overwash fans
336 [e.g., *Fisher et al.*, 1974; *Leatherman et al.*, 1977; *Leatherman and Zaremba*, 1987]. Because
337 *GEOMBEST+* provides a representation of the accumulation of overwash deposits over the span
338 of a given time, we do not select values for overwash thickness (A_{OW0}) to reflect the thickness of
339 individual overwash fans measured in the field, but rather to reflect the thickness of all the
340 overwash deposits from a given period of time. For this reason, we hold A_{OW0} constant at 1/200th
341 of the Q_{OW} value, keeping the length of the overwash fan constant, representing the average

length of a fan that would result from multiple storms of similar scale. This parameterization results in an average overwash slope, of 0.005 dipping toward the backbarrier, which falls in the range of measured values (0.001-0.02) [*Leatherman et al.*, 1977], and overwash extents of up to 200m, which is also within the range of observed values (90 -~400m)[*Fisher et al.*, 1974; *Leatherman et al.*, 1977; *Leatherman and Zaremba*, 1987].

2.3.4 Bay Parameterizations and Relative Sea Level Rise Rates

We vary bay sediment flux (Q_B) across a range of values from 2 to 20 m^3/m/yr (Table 1). This parameter is not well constrained, so a range of 2-20 m^3/m/yr is used to explore the response of the coupled system to variations in sediment input from bays. We set the maximum bay erosion rate (E_{max}) to 10 cm/yr, and the resuspension depth (d_R) to 0.4 meters (Table 1). These values are determined empirically through *GEOMBEST+* simulations in order to constrain the bay to a range of morphological behavior appropriate for a shallow backbarrier bay. (Note: These parameters can be calibrated to approximate larger bays that generate larger waves with an increased potential for sediment resuspension.)

We consider *R* values ranging from 1 to 10 mm/yr (in increments of 1) to include and (because there is uncertainty in future rates) expand upon the range of relative sea level rise rates observed for the East Coast region of the United States [*Engelhart et al.*, 2009; *Sallenger et al.*, 2012]. We vary the *R* such that sea level rises a total of 1 m in each simulation, resulting in simulated time periods ranging from 100 to 1000 years. Constraining total sea level rise in this way ensures that the barrier island traverses the same stretch of substrate in each simulation, thereby controlling for the effect of the antecedent substrate slope on barrier island migration [*Moore et al.*, 2010]. Although allowing simulations having low *R*s to run longer than simulations having high *R*s allows for more deposition to occur in the longer simulations

compared to the shorter simulations, deposition occurs at the same rate in all cases. This would not be the case if all simulations instead have the same duration, because flooding of upland areas due to sea level rise can lead to changes in backbarrier basin width which can alter the rate of deposition across a basin. Since it is the competition between the rates of sea level rise and deposition (instead of the cumulative totals of each) that determine the change in elevation relative to seal level, we chose to keep total sea level rise constant, and therefore control for variation in the deposition rates.

2.4 Model Inputs for Island-Migration Experiments

In addition to investigating the impact of island migration on backbarrier marsh morphology, we conduct a set of 1000-year-long experiments using *GEOMBEST+* to assess how long-term island migration rates change across barrier-marsh systems having different marsh widths and sediment characteristics (i.e., sand content and erodibility). We use the same inputs for initial morphology and stratigraphy, marsh sand and organic content, E_{max}, and d_R as described above. Because these long-term (1,000 years) experiments are designed to assess the effect of differences in backbarrier environment (morphology and sand content) on island migration, we hold R constant at 4 mm/yr, selected to approximate the average rate of RSLR observed in the Virginia Coast Reserve [*Porter et al.*, 2013] over the past century. This value is consistent with conservative projections according to *IPCC* [2014]. To represent different backbarrier morphologies and sand contents, we vary Q_B and Q_{OW} within a range of values chosen based on the results from the marsh-width experiments (Table 2; see: section 3.2 for further discussion of parameterization).

3. Simulation Results and Comparison with Observations

3.1 Impact of Barrier and Backbarrier Processes on Marsh Width

3.1.1 Marsh-Width Experiments

For the marsh width experiments (described in section 2.3), the distance from the dune limit to the landward extent of the marsh platform (i.e., marsh width) is measured at the end of each simulation. Using this output, we then compute the frequency distribution of final marsh widths resulting from all experiments. If a given backbarrier marsh width is stable in the model, meaning that the progradation rate at the marsh boundary is equal to the landward migration rate of the island, then marshes of that particular width should occur with a greater frequency than others. The frequency distribution of final backbarrier marsh width from the experiments shows that there are peaks at both 0 m and 2000 m, representing backbarrier basins that are completely empty and completely filled with marsh (Figure 4A), respectively. The marsh-filled peak includes values above the initial maximum backbarrier marsh width (1800 m), because part of the mainland is submerged by rising sea level, allowing the marsh to expand into the mainland faster than the barrier migrates landward. The inner boundary of each of the two end-member peaks is determined as the point of maximum deviation from a hypothetical random uniform distribution (67 m for the empty-basin peak and 1775 m for the marsh-filled peak; Figure 4B). We then remove from the dataset all width values associated with the empty-basin and filled-basin peaks to test the null hypothesis that the remaining widths are uniformly distributed, i.e., that each bin has an equal probability of marshes occurring in that width. This analysis yields a third peak that is smaller than the two end member peaks, and is centered at approximately 300 meters (Figure 4C). A one-sample Kolmogorov–Smirnov test for statistical significance confirms that the intermediate peak deviates from a random uniform distribution (99% confidence level),

412 with the maximum deviation occurring at 448 m, setting the upper bound of the intermediate
413 peak range (Figure 4D). The lower bound is set to the point at which the empirical distribution
414 begins to deviate from the uniform distribution, at approximately 150 m (Figure 4D). This leads
415 to the identification of a statistically significant intermediate peak at 150-450 m, centered on a
416 width of 300 m, suggesting that marshes may be stable at this width.
417 To test the stability of narrow marshes, we run the simulations that result in final marsh
418 widths in the range of 150-450 m for an additional meter of sea level rise, holding the parameters
419 for Q_{OW}, Q_B, and R constant. Of the 340 runs (11.3% of all simulations) that populate the narrow
420 marsh peak after one meter of sea level rise, only 33 remain in the 150-450m range after an
421 additional meter of sea level rise (Figure 5), suggesting a sensitivity of narrow marshes in model
422 simulations to the total amount of sea level rise. Backbarrier marsh width decreases sharply for
423 the initially filled basins at 0.5-0.7m of sea level rise, due to the formation of a small (50-100m;
424 1-2 cells) bay in the middle of the marsh platform, based on our assumption that a new drainage
425 basin would form in the middle of a large marsh platform. In the simulations that begin with an
426 initially empty basin, the backbarrier marsh progrades throughout the simulation, passing
427 through the narrow marsh range and ultimately stabilizing once the entire basin is filled. In
428 simulations beginning with initially narrow or initially filled basins, marshes decrease in width
429 throughout the simulation, only stabilizing once marsh width becomes zero, as it does for > 90%
430 of these marshes (Figure 5). However, because there is a statistically significant peak in the
431 occurrence of narrow marshes after one meter of sea level rise which represents the passing of a
432 substantial period of time, the narrow marsh is a high probability state in the model. Therefore,
433 the narrow marsh peak represents a long-lasting transient state which results in a higher than
434 expected frequency of narrow marshes for an extended duration.

435 Altogether, there are three states in which backbarrier marshes in the model tend to reside
436 with a statistically-significant high frequency (i.e., they are alternate states): empty (< 67m),
437 filled (> 1775m), and narrow (150-450m). Comparison of the values for Q_{OW}, Q_B, and R
438 associated with the occurrence of marshes in the range of widths representing each alternate state
439 allows us to constrain the conditions that lead to each potential state (Figure 6). Q_B is negatively
440 correlated with the occurrence of empty basins (m = -1.4) and marshes in the narrow width range
441 (m = -0.95), and it is strongly positively correlated with the occurrence of basins filled with
442 marsh (m = 0.75) (Figure 6A). Relationships with R show the opposite of those for Q_B (Figure
443 6B): R is positively correlated with the occurrence of empty basins (m = 2.5) and narrow
444 marshes (m = 1.3), and negatively correlated with filled basins (m = -1.3). Q_{OW} appears to be
445 slightly positively correlated with the occurrence of marshes in the range of full basins (m =
446 0.22), but is strongly positively correlated with the occurrence of narrow marshes (m = 1.9) and
447 strongly negatively correlated with the occurrence of empty basins (Figure 6C). Thus, Q_B and R
448 appear to be the most important factors in maintaining filled and empty basins within the model,
449 while Q_{OW} appears to play a more important role in the occurrence of narrow marshes.
450 Another way to visualize the different alternate states and the conditions leading to them is to
451 consider how marsh width changes across the parameter space. Generally, marsh width increases
452 as R decreases and Q_B increases, such that the accretion of fine-grained sediment delivered to the
453 bay is equal to the increase in accommodation resulting from rising sea level. The basin
454 accretion rate (hereafter referred to as *BAR*) is equal to the Q_B divided by the basin width (2000
455 m). The ratio of *BAR* to R thus provides an index by which to measure changes in marsh width:
456 values greater than one lead to marsh progradation and thus wider marshes whereas values less
457 than one lead to marsh erosion and narrower marshes. This is observed in model results which

458 suggest that initially empty basins remain empty for nearly all *BAR*/*R* ratios less than 1, except in
459 the case of high overwash volume fluxes, where some narrow marshes (width = ~150-500 m)
460 occur at ratios just between 0.9 and 1 (yellow zone falling just below the dashed line; Figure
461 7A). In the case of marshes that are initially narrow, marsh width is maintained under a wider
462 range of conditions than in the case of initially empty basins (Figure 7B). Marsh width in basins
463 that begin marsh-filled is maintained at even lower *BAR*/*R* ratios than in either of the other cases,
464 whereas the instance of no marsh occurs at very low *BAR*/*R* ratios, but only at low values of
465 overwash volume flux (Figure 7C). Combining in the parameter space all simulations that lead to
466 one of the three states (Figure 7D), highlights that all states can occur at *BAR*/*R* ratios from 0.9 to
467 1, and that the range of conditions in which narrow marshes and empty basins are meta-stable
468 and stable, respectively, overlaps considerably. This suggests that the initial width of a marsh
469 may be important in determining its stability: differences in initial marsh width can lead to
470 differences in the state that marsh width converges on, highlighting the legacy of initial
471 conditions in barrier island evolution [e.g., *Perron and Fagherazzi*, 2012].
472
473 *3.1.2 Comparison of Experimentally-derived Marsh Widths to Observations from Remote*
474 *Sensing*
475 Results from model simulations suggest the existence of three long-lasting alternate states in
476 backbarrier marsh width relative to basin size: empty basins (marsh width = 0 m), basins
477 partially filled by marshes of narrow width (marsh width = 150 – 450 m), and basins that are
478 completely filled by marsh (marsh width = basin width). This leads to a testable hypothesis that
479 there are more backbarrier marshes in the VBIs having widths within these ranges than in others.
480 To test this prediction, we use satellite imagery to measure the width of backbarrier marshes
481 along the VBIs. Within the VBIs, relative sea level rise rate is uniform, but fine-grained sediment

supply, overwash fluxes, backbarrier basin area, and historical backbarrier marsh width are variable, which could lead to the existence of multiple stable or transient states within this one geographic location (e.g., Figure 7D).

To calculate marsh width we used ASTER satellite imagery (resolution = 15m) from the U.S. Geological Survey (*USGS)* [2010] . We selected images acquired at mid-day during low tide and during peak growing season in order to maximize the visibility of the vegetated marsh platform [*Hinkle and Mitsch*, 2005]. We classified marsh on the basis of threshold values for the Normalized Difference Vegetation Index (NDVI) and the three 15 m resolution visible and near-infrared bands [*Xie et al.*, 2008]. For the purpose of this study, we define backbarrier marsh width as the straight line distance from the location where marsh vegetation first appears behind the barrier island to the nearest non-marsh point (greater than 50 m) along a transect perpendicular to the marsh/island boundary. The nearest non-marsh point can be either an open water bay or the mainland in the case of a backbarrier basin that is completely filled with marsh. We collected measurements of backbarrier marsh width at 15-m increments alongshore, excluding areas within 1 km of an inlet, to avoid the inclusion of flood tidal deltas.

The resulting frequency distribution of observed backbarrier marsh widths for Metompkin Island exhibits three peaks (Figure 8). Peaks associated with the boundaries of the backbarrier basin occur from 0-100 m and 1900-2000 m (in line with model predictions) with an intermediate peak centered at 425 m (range = 150-700 m), which overlaps with the range of the peak identified in model results (range = 150-450 m). We then normalized to basin width by dividing marsh width by basin width and multiplying by 2000 m, such that all basins filled with extensive marsh platforms plot at 2000 m.

504 The resulting frequency distribution of backbarrier marsh width for all islands in the VBIs
505 (Figure 9A), normalized to basin width, shows a distinct peak at the upper boundary associated
506 with filled basins, but no peak associated with the lower boundary, where the frequency of width
507 measurements is actually less than that predicted by a random uniform distribution (Figure 9B).
508 Removing the widths associated with the boundary conditions, and testing the intermediate peak
509 in the 150-700 m range for statistical significance using the Kolmogorov–Smirnov test, shows
510 that the peak deviates from the predicted random uniform distribution (99% confidence level)
511 (Figure 9D) strongly suggesting that the deviation is not random, but rather associated with some
512 process that produces more marshes in that range of widths than in others. In comparing model
513 results to these observations of natural marshes we put more emphasis on the fact that peaks exist
514 in both cases rather than on a quantitative comparison of the ranges of marsh widths within the
515 peaks.
516
517 ***3.2 Impact of Backbarrier Environment on Long-Term Island Migration Rates***
518 For the long-term island migration experiments, we hold backbarrier marsh width constant at
519 one of the three observed alternate states (empty basin, narrow marsh, or filled basin) by
520 selecting the appropriate parameters to maintain the width of the marsh (Table 2). For each of
521 these three states, we then vary the relative contribution to the marsh from sand delivered via
522 overwash (Q_{OW}) versus fine-grained sediment exported from the bay (Q_B). The marsh
523 sedimentology changes as a result of the relative contribution of sediment from different sources,
524 ranging from a marsh-filled basin maintained almost exclusively by fine-grained sediment input
525 from bay sediment flux (Q_B = 16 m^3/m/yr ; Q_{OW} = 0.5 m^3/m/yr) to an empty basin having a large
526 contribution from overwash volume flux (Q_B = 4 m^3/m/yr ; Q_{OW} = 2 m^3/m/yr,Table 2). Varying
527 sediment inputs to the marsh in this way leads to the development of marsh layers (as marsh

528 accumulates throughout each run) that vary in sand content (ranging from muddy to sandy)
529 across the simulations. We also run each pair of values for marsh width and relative contribution
530 from the two sediment sources with different erodibilities for the marsh stratigraphic unit (0.01,
531 0.1, 0.5 and 1) (Table 1) resulting in a suite of 36 simulations.

532 Model results suggest that island migration rate increases as the sand content of the marsh
533 increases, because the increase in sand content is a result of an increase in Q_{OW}, which ultimately
534 increases the rate that sand is lost from the front of the island. This increased sand loss results in
535 an increase in the rate of shoreface erosion, although ultimately the overwash sand can be re-
536 excavated from the shoreface once the barrier migrates over the marsh. Overall, however, marsh
537 width plays the more dominant role in controlling island migration rate. Results suggest that, in
538 general, migration rates are higher for islands backed by empty basins, and lower for islands
539 backed by basins filled with marsh (Figure 10). This is quantified in the relationship between
540 island migration rate and Q_B: total island migration over the course of the experiment is reduced
541 by 35 m with the addition of 1 m^3/m/yr of Q_B (holding all other variables constant), or, put a
542 different way, island migration rate decreases by 30% for islands backed by filled basins
543 compared to islands backed by empty basins. Comparatively, island migration increases by 2 m
544 over the 1,000 year simulation with the addition of 1 m^3/m/yr of Q_{OW}, or island migration rate
545 increases 8.5% for islands having a higher rate of overwash compared to islands having a lower
546 rate of overwash (Table 2). Consistent with results of *Moore et al.* [2010], erodibility of the
547 marsh stratigraphic unit appears to have a negligible effect on island migration rate.
548
549

4. Discussion

4.1 Model Limitations

GEOMBEST+ operates in 2 dimensions (cross-shore), and is therefore unable to address alongshore heterogeneities such as alongshore variations in shoreline erosion or overwash deposition, which tends to occur preferentially in areas where dunes are lower. This can be especially important in areas where ecomorphodynamic feedbacks may cause low areas to remain low longer, thereby increasing alongshore heterogeneity in susceptibility to future overwash events [*Hosier and Cleary*, 1977; *Fagherazzi and Priestas*, 2012; *Wolner et al.*, 2013]. However, the model does provide useful insights into the cross-shore processes of barrier island systems.

Overwash is set as a fixed parameter in *GEOMBEST+*, which allows us to investigate the effect of overwash as an independent variable. In nature, however, overwash itself will vary with barrier island geometry such that wider, higher islands will tend to experience less overwash. Addressing the effect of island geometry on overwash is beyond the scope of the work presented here, but recent work by *Lorenzo-Trueba and Ashton* [2014] addressing this effect concludes that the couplings between overwash flux and barrier geometry can result in barrier island drowning when overwash is insufficient to maintain barrier height.

GEOMBEST+ captures the impact of depositional events that take the marsh out of its preferred elevation range, because marsh will only grow in the model below the high water line. However, the relationship between depth and the rate of marsh growth is not described in the current version of the model. As a result, within the model, the marsh accretes at a rate that depends only on the supply of sediment (sand and fine-grained), and accretion rate does not increase as the depth below high tide increases as it should, based on findings of e.g., *Morris et*

573 *al.* [2002] and *Kirwan et al.* [2010]. This feedback would serve to extend the range of conditions
574 under which marsh platforms—created under conditions of favorable sea level rise and sediment
575 input conditions—are stable as RSLR rate increases and fine-grained sediment supply decreases.
576 However, this ecomorphodynamic feedback is not important for the scope of this research, as it
577 does not directly impact the rate of creation of new marsh at the bay-marsh boundary.
578 Finally, in our simple formulation we have not implemented wave erosion of the marsh
579 boundary [e.g., *Mariotti and Fagherazzi* 2010]. The addition of wave erosion, as a function of
580 bay fetch, would likely result in a higher frequency of the empty and marsh-filled potential stable
581 states. This is because the reduction in wave heights in a small basin, and the increase in wave
582 heights in large basins, would cause negative feedbacks that tend to maintain these conditions.
583
584 ***4.2 Impact of Overwash on Backbarrier Marshes***
585 In our numerical experiments, the occurrence of marshes in the range of narrow marsh
586 widths that made up the previously identified statistically significant peak is positively correlated
587 with the parameter for overwash volume (Figure 6). This suggests that overwash plays a critical
588 role in allowing the bay-marsh boundary to prograde ahead of the landward migration of the
589 marsh-barrier boundary under a range of conditions (i.e., high R and low Q_B) when we would
590 otherwise expect no marsh to exist. Overwash also appears to provide marshes with a valuable
591 source of sediment which helps to counteract the effects of sea level rise. Because overwash
592 deposition is limited in extent, marshes having an insufficient supply of fine-grained sediment to
593 prograde beyond the zone in which overwash has influence will tend to be narrow. Once the bay-
594 marsh boundary of a narrowing marsh enters the overwash zone, overwash deposition will allow
595 the bay-marsh boundary to begin prograding again (which only leads to the marsh widening if
596 progradation outpaces landward migration of the marsh-barrier boundary). However, model

results suggest that these narrowing marshes are only temporarily stabilized by overwash and that they will continue to narrow and ultimately disappear. This is in agreement with the results of *Mariotti and Fagherazzi* [2010], which suggest that a stable state between the empty and marsh-filled basins does not exist but that marshes, instead, are constantly adjusting by narrowing or widening. Adding to the findings of *Mariotti and Fagherazzi* [2010], model results from *GEOMBEST+* suggest that a narrow marsh alternate state can occur with a higher-than-expected frequency under conditions of either bay-marsh boundary progradation (i.e., starting from an initially empty basin) or bay-marsh erosion (i.e., starting from an initially marsh-filled or narrow marsh condition), provided that a source of sediment from overwash is present, although this state is transient and narrow marshes will ultimately disappear or become marsh-filled basins (Figure 5). In the case of marsh-filled basins transitioning to narrow marshes, it appears that the initial marsh height determines the timing of the transition, as the marsh drowns in the center after just over 0.5m of sea level rise (Figure 5), a number that is likely a result of model initial conditions and parameterization, and is not indicative of what we would expect for real world marshes. However, though in all cases the narrow marsh state appears transient in model results, it is possible that in the case of a marsh prograding from an initially empty basin that addition of wave erosion and changing boundary conditions to allow export of fine-grained sediment could lead to a stabilization of the marsh boundary.

Our results predict the range of marsh widths observed for the VBIs, which fall into the range of values represented in the lower right quadrant of Figure 7C, where both the narrow marsh and marsh-filled basin states are prevalent. The VBIs experience a uniform RSLR rate, and though rates of basin accretion likely vary, the region is generally sediment deficient and likely in an approximate range of $BAR/R = 0.1 – 1$ (Figure 7). Smaller backbarrier basins likely fall closer to

620 the upper range of *BAR/R* values, where marsh-filled basins are stable, and larger basins are
621 more likely to fall toward the lower range, where narrow marshes are stable. Because the VBIs
622 are generally low-lying and landward-migrating (and thus experience relatively high overwash
623 flux), the existence of a narrow marsh transient state is not surprising and suggests that marsh-
624 filled basins may have been prevalent here in the past—either due to lower RSLR rates or higher
625 fine-grained sediment supply, or some combination of the two—and are in the process of
626 transitioning to an empty basin stable state.

627 In a recent study of several overwash fans on Martha's Vineyard, MA by *Carruthers et al.*
628 [2013] overwash fluxes were found to be up to several times higher (2-8 m^3/m/yr) than the
629 maximum values used in simulations here. Given this finding, along with the potential for
630 increased storm intensity and therefore increased overwash flux in the future, it is worth
631 considering the effect of higher overwash fluxes on the barrier island-marsh couplings. Thus, we
632 ran a few additional exploratory simulations at Q_{OW} values of up to triple (6 m^3/m/yr) the
633 maximum overwash values investigated in the marsh-width experiments and found the same
634 trends as shown at lower overwash fluxes. Initially empty basins remain empty despite very large
635 overwash fluxes, and initially filled basins tend to transition to narrow marshes under conditions
636 where R outpaces Q_B. However, narrow marshes appear to persist longer under the higher Q_{OW},
637 suggesting perhaps that with a high enough supply of sediment from overwash, backbarrier
638 marshes could be stabilized under fine-grained sediment deficient conditions. Because our
639 results (Figures 6 and 7) suggest that overwash increases the prevalence of narrow backbarrier
640 marshes, we expect that as overwash flux increases, the range of conditions (of R and Q_B) under
641 which narrow backbarrier marshes could persist would broaden.

642 It is important to recognize that in addition to the role of Q_{OW}, Q_B, and R, the proportion of
643 the backbarrier that is filled with marsh varies greatly depending on many parameters—both in
644 the model and in reality—beyond the most important parameters explored here. For example, the
645 width of the backbarrier bay plays an important role by increasing accommodation, which leads
646 to enhanced deposition of fine-grained sediment in the bay and relatively less deposition of fine-
647 grained sediment on the marsh. Similarly, it appears that island migration rate also causes
648 variations in marsh width, as suggested by two runs which result in the same marsh progradation
649 rate, but different island transgression rates (Figure). In the case of more rapid island
650 transgression, the marsh is narrower, because the island rolls over and destroys the trailing edge
651 of the marsh, consistent with observations made from aerial photographs by *Kastler and Wiberg*
652 [1996].
653 Overwash also likely has additional impacts on backbarrier marshes not considered herein. In
654 the model, overwash deposition always occurs as a layer on top of the backbarrier marsh
655 platform or bay floor. However, field observations and stratigraphic studies of overwash fans
656 have shown that, in some cases, overwash actually scours pre-existing sedimentary layers before
657 depositing sand on top, in some cases causing net erosion. [e.g., *Fisher et al.*, 1974; *Wang and*
658 *Horwitz*, 2007]. Further, scouring and burial by overwash have the potential to destabilize the
659 marsh platform by removing and smothering marsh vegetation [*Kirwan et al.*, 2008; *Temmerman*
660 *et al.*, 2012].
661
662 **4.3 Impact of Marsh Morphology and Sedimentology on Island Migration**
663 Islands backed by marshes have the added benefit of reduced accommodation, which allows
664 an island to remain “perched” on the marsh, compared to islands backed by open bays, which
665 must migrate farther landward to maintain elevation relative to sea level. This has broad

implications for our understanding of how barrier island migration varies alongshore. All other geologic constraints being equal, marsh-backed islands appear less vulnerable to rising sea level than bay-backed islands, because they are able to maintain a more offshore position without a significant contribution of sand from alongshore transport or the shoreface.

Turning to the VBIs for examples, the reduction in vulnerability of marsh-backed islands may explain the lower migration rate of the marsh-backed northern half of Metompkin Island relative to the bay-backed southern half [*Byrnes*, 1988], as well as the persistence of the southern islands in the VBIs, which are low-lying, marsh-backed and sediment-starved [*Demarest and Leatherman*, 1985], but have not yet transitioned into the "runaway transgression" phase [*FitzGerald et al.*, 2006].

Results also indicate that, in the short term, islands backed by sandy marshes that experience an increase in overwash will initially migrate landward faster due to the removal of sand from the shoreface associated with overwash deposition. This is consistent with the conventional view that overwash is associated with an increase in the landward rate of island migration, as the erosion of sand from the shoreface and deposition in the backbarrier results in net landward migration of the island [e.g., *Stolper et al.*, 2005; *Moore et al.*, 2010]. However, model results presented here also suggest that for scenarios in which an increase in overwash leads to the maintenance of narrow marshes (versus disappearance or absence of marsh), landward rates of island migration in the long term may be reduced because the decrease in migration rate resulting from the reduction in accommodation afforded by the presence of a marsh is greater than the increase in migration rate associated with overwash processes. In this way, there appears to be a potentially symbiotic feedback between landwardly-migrating barrier islands and narrow sandy marshes, whereby the reduction in accommodation afforded by the marsh increases island

689 stability and the contribution of overwash sediment from the island helps the marsh to keep pace
690 with sea level.
691
692 **5. Conclusions**
693 Here, we develop *GEOMBEST+*—which simulates the coupled dynamic evolution of barrier
694 islands and backbarrier marshes—and apply it to investigate the complexities of island-marsh co-
695 evolution. Results from model experiments suggest that overwash deposition is important in the
696 maintenance of transient narrow marsh platforms under conditions of low fine-grained sediment
697 supply and high relative sea level rise rates under which they otherwise would not occur. This
698 conclusion is supported by observations of marsh width from satellite imagery, which reveal a
699 peak in the frequency of marshes in this narrow width range.
700 Model experiments of long-term barrier island migration suggest that islands backed by
701 marsh platforms have migrate landward more slowly because the presence of a marsh reduces
702 accommodation behind the island. In conditions of high RSLR rate and low fine-grained
703 sediment input from the associated bay, the presence of overwash appears necessary to maintain
704 a narrow backbarrier marsh, which in turn decreases the rate of island retreat. Taken together,
705 our results suggest that feedbacks between barrier island and backbarrier environments influence
706 the evolution of barriers and marshes. Such feedbacks may become increasingly important in
707 determining the fate of island systems in the future as hurricanes become more frequent and/or
708 more intense and as sea level continues to rise in response to climate change.
709

Acknowledgements

We thank JGR-ES Editor Alex Densmore, Associate Editor Andrew Ashton, Jorge Lorenzo Trueba and 2 anonymous reviewers for thoughtful comments and suggestions that

improved this manuscript. We also thank A. Brad Murray and Larry Benninger for helpful comments on an early draft of this work. Funding was provided by the Department of Geological Sciences Martin Fund at the University of North Carolina Chapel Hill (UNC-CH) and by the Virginia Coast Reserve Long-Term Ecological Research Program (National Science Foundation Grant DEB–1237733) via a subaward from the University of Virginia to the UNC-CH. The data for this paper are available by contacting David Walters at dcwalters@vims.edu.

References

Belknap, D., and J. Kraft (1985), Influence of antecedent geology on stratigraphic preservation potential and evolution of Delaware's barrier systems, *Mar. Geol., 63,* 235–262, doi:0025-3227/85.

Bender, M.A., T.R. Knutson, R.E. Tuleya, J.J. Sirutis, G.A. Vecchi, S.T. Garner, and I.M. Held (2010), Modeled impact of anthropogenic warming on the frequency of intense Atlantic hurricanes., *Science, 327,* 454–458, doi:10.1126/science.1180568.

Boothroyd, J., N. Friedrich, and S. McGinn (1985), Geology of microtidal coastal lagoons: Rhode Island, *Mar. Geol., 63,* 35–76, doi:0025-3227/85.

Brenner, O.T. (2012), The Complex Influences of Backbarrier Deposition, Substrate Slope and Underlying Stratigraphy in Barrier Island Response to Sea Level Rise: Insights from the Virginia Barrier Islands, Mid-Atlantic Bight, U.S.A., M.S. thesis, University of Virginia, Charlottesville, Va.

Bruun, P. (1988), The Bruun rule of erosion by sea-level rise: a discussion on large-scale two- and three-dimensional usages, *J. Coast. Res., 4,* 627–648, doi:88001.

Byrnes, M.R. (1988), Holocene geology and migration of a low-profile barrier island system, Metompkin Island, Virginia., M.S. thesis, Old Dominion University, Charlottesville, Va.

Cahoon, D., and D. Reed (1995), Relationships among marsh surface topography, hydroperiod, and soil accretion in a deteriorating Louisiana salt marsh, *J. Coast. Res., 11,* 357–369, doi:4298345.

Carruthers, E.A., D.P. Lane, R.L. Evans, J.P. Donnelly, and A.D. Ashton (2013), Quantifying overwash flux in barrier systems: An example from Martha's Vineyard, Massachusetts, USA, *Mar. Geol., 343,* 15–28, doi:10.1016/j.margeo.2013.05.013.

Chmura, G., and G. Hung (2004), Controls on salt marsh accretion: A test in salt marshes of Eastern Canada, *Estuaries, 27,* 70–81, doi:1353491.

Costanza, R., R. Arge, R. De Groot, S. Farberk, M. Grasso, B. Hannon, K. Limburg, S. Naeem, R.V.O. Neill, J. Paruelo, R.G. Raskin, and P. Suttonkk (1997), The value of the world's ecosystem services and natural capital, *Nature, 387,* 253–260, doi:10.1038/387253a0.

Demarest, J., and S. Leatherman (1985), Mainland influence on coastal transgression: Delmarva Peninsula, *Mar. Geol., 63,* 19–33, doi:0025-3227.

Emanuel, K.A. (2013), Downscaling CMIP5 climate models shows increased tropical cyclone activity over the 21st century, *Proc. Natl. Acad. Sci. U. S. A.*, *110*, 12219–12224, doi:10.1073/pnas.1301293110.

Engelhart, S.E., B.P. Horton, B.C. Douglas, W.R. Peltier, and T.E. Tornqvist (2009), Spatial variability of late Holocene and 20th century sea-level rise along the Atlantic coast of the United States, *Geology*, *37*, 1115–1118, doi:10.1130/G30360A.1.

Fagherazzi, S., and A.M. Priestas (2012), Back-barrier flooding by storm surges and overland flow, *Earth Surf. Process. Landforms*, *37*, 400–410, doi:10.1002/esp.2247.

Fagherazzi, S., L. Carniello, L. D'Alpaos, and A. Defina (2006), Critical bifurcation of shallow microtidal landforms in tidal flats and salt marshes, *Proc. Natl. Acad. Sci. U. S. A.*, *103*, 8337–8341, doi:10.1073?pnas.0508379103.

Fisher, J., S. Leatherman, and F. Perry (1974), Overwash processes on Assateague Island, *Coast. Eng.*, 1194–1212, doi:10.9753/icce.v14.

FitzGerald, D., I. Buynevich, and B. Argow (2006), Model of tidal inlet and barrier island dynamics in a regime of accelerated sea level rise, *J. Coast. Res., II*, 789–795, doi:0749-0208.

French, J. (1993), Numerical simulation of vertical marsh growth and adjustment to accelerated sea-level rise, North Norfolk, UK, *Earth Surf. Process. Landforms*, *18*, 63–81, doi:0197-9337.

Gunnell, J.R., A.B. Rodriguez, and B.A. McKee (2013), How a marsh is built from the bottom up, *Geology*, *41*, 859–862, doi:10.1130/G34582.1.

Hinkle, R.L., and W.J. Mitsch (2005), Salt marsh vegetation recovery at salt hay farm wetland restoration sites on Delaware Bay, *Ecol. Eng.*, *25*, 240–251, doi:10.1016/j.ecoleng.2005.04.011.

Hosier, P., and W. Cleary (1977), Cyclic geomorphic patterns of washover on a barrier Island in southeastern North Carolina, *Enivronmental Geol.*, *2*, 22–31, doi:10.1007/BF02430662.

Hoyt, J. (1967), Barrier island formation, *Geol. Soc. Am. Bull.*, *78*, 1125–1136, doi:10.1130/0016-7606(1967)78.

IPCC (2014), 2013: Sea Level Change. In Climate Change 2013: The Physical Science Basis. Contribution of Working Group I to the Fifth Assessment Report of the Intergovernmental Panel on Climate Change, (New York, NY, USA: Cambridge University Press),.

Kastler, J.A., and P.L. Wiberg (1996), Sedimentation and Boundary Changes of Virginia Salt Marshes, *Estuar. Coast. Shelf Sci.*, *42*, 683–700, doi:10.1006/ecss.1996.0044.

Kirwan, M., A. Murray, and W. Boyd (2008), Temporary vegetation disturbance as an explanation for permanent loss of tidal wetlands, *Geophys. Res. Lett.*, *35*, 1–5, doi:10.1029/2007GL032681.

Kirwan, M.L., G.R. Guntenspergen, A. D'Alpaos, J.T. Morris, S.M. Mudd, and S. Temmerman (2010), Limits on the adaptability of coastal marshes to rising sea level, *Geophys. Res. Lett.*, *37*, 1–5, doi:10.1029/2010GL045489.

Kirwan, M.L., A.B. Murray, J.P. Donnelly, and D.R. Corbett (2011), Rapid wetland expansion during European settlement and its implication for marsh survival under modern sediment delivery rates, *Geology*, *39*, 507–510, doi:10.1130/G31789.1.

Knutson, T.R., J.L. McBride, J. Chan, K. Emanuel, G. Holland, C. Landsea, I. Held, J.P. Kossin, a. K. Srivastava, and M. Sugi (2010), Tropical cyclones and climate change, *Nat. Geosci.*, *3*, 157–163, doi:10.1038/ngeo779.

Leatherman, S., and R. Zaremba (1987), Overwash and aeolian processes on a US northeast coast barrier, *Sediment. Geol.*, *52*, 183–206, doi:0037-0738(87)90061-3.

Leatherman, S., A. Williams, and J. Fisher (1977), Overwash sedimentation associated with a large-scale northeaster, *Mar. Geol.*, *24*, 109–121, doi:10.1016/0025-3227(77)90004-4.

Lorenzo-Trueba, J., and A. Ashton (2014), Rollover, drowning, and discontinuous retreat: Distinct modes of barrier response to sea-level rise arising from a simple morphodynamic model, *J. Geophys. Res. Earth Surf.*, 1–23, doi:10.1002/2013JF002941.

Mariotti, G., and S. Fagherazzi (2010), A numerical model for the coupled long-term evolution of salt marshes and tidal flats, *J. Geophys. Res. Earth Surf.*, *115*, F01004, doi:10.1029/2009JF001326.

Mariotti, G., S. Fagherazzi, P.L. Wiberg, K.J. McGlathery, L. Carniello, and A. Defina (2010), Influence of storm surges and sea level on shallow tidal basin erosive processes, *J. Geophys. Res.*, *115*, C11012, doi:10.1029/2009JC005892.

Masetti, R., S. Fagherazzi, and A. Montanari (2008), Application of a barrier island translation model to the millennial-scale evolution of Sand Key, Florida, *Cont. Shelf Res.*, *28*, 1116–1126, doi:10.1016/j.csr.2008.02.021.

Moore, L.J., J.H. List, S.J. Williams, and D. Stolper (2010), Complexities in barrier island response to sea level rise: Insights from numerical model experiments, North Carolina Outer Banks, *J. Geophys. Res.*, *115*, F03004, doi:10.1029/2009JF001299.

Morris, J., P. Sundareshwar, C. Nietch, and B. Kjerfve (2002), Responses of coastal wetlands to rising sea level, *Ecology*, *83*, 2869–2877, doi:10.1890/0012-9658(2002)083[2869:ROCWTR]2.0.CO;2.

Mudd, S.M. (2011), The life and death of salt marshes in response to anthropogenic disturbance of sediment supply, *Geology*, *39*, 511–512, doi:10.1130/focus052011.1.

Mudd, S.M., A. D'Alpaos, and J.T. Morris (2010), How does vegetation affect sedimentation on tidal marshes? Investigating particle capture and hydrodynamic controls on biologically mediated sedimentation, *J. Geophys. Res.*, *115*, F03029, doi:10.1029/2009JF001566.

Osgood, D.T., and J.C. Zieman (1993), Spatial and Temporal Patterns of Substrate Physiochemical Parameters in Different-aged Barrier Island Marshes, *Esuarine, Coast. Shelf Sci.*, *37*, 421–436, doi:10.1006/ecss.1993.1065.

Perron, J.T., and S. Fagherazzi (2012), The legacy of initial conditions in landscape evolution, *Earth Surf. Process. Landforms*, *37*, 52–63, doi:10.1002/esp.2205.

Porter, J., D. Krovetz, J. Spitler, T. Williams, and K. Overman (2013), Tide Data for Hog Island (1991-), Redbank (1992-), Oyster (2007-). 12 minute interval., *Long-Term Ecol. Res. Proj. Data Publ.*, Virginia Coast Reserve,.

Riggs, S.R., W.J. Cleary, and S.W. Snyder (1995), Influence of inherited geologic framework on barrier shoreface morphology and dynamics, *Mar. Geol.*, *126*, 213–234, doi:0025-3227.

Rodriguez, A.B., S.R. Fegley, J.T. Ridge, B.M. VanDusen, and N. Anderson (2013), Contribution of aeolian sand to backbarrier marsh sedimentation, *Estuar. Coast. Shelf Sci.*, *117*, 248–259, doi:10.1016/j.ecss.2012.12.001.

Sallenger, A., K. Doran, and P. Howd (2012), Hotspot of accelerated sea-level rise on the Atlantic coast of North America, *Nat. Clim. Chang.*, *2*, 884–888, doi:10.1038/nclimate1597.

Stolper, D., J.H. List, and E.R. Thieler (2005), Simulating the evolution of coastal morphology and stratigraphy with a new morphological-behaviour model (GEOMBEST), *Mar. Geol.*, *218*, 17–36, doi:10.1016/j.margeo.2005.02.019.

Storms, J., G. Weltje, and J. Van Dijke (2002), Process-response modeling of wave-dominated coastal systems: simulating evolution and stratigraphy on geological timescales, *J. Sediment. Res.*, *72*, 226–239, doi:1527-1401/02/072-226.

Swift, D. (1975), Barrier-Island Genesis: Evidence from the Central Atlantic Shelf, Eastern U.S.A., *Sediment. Geol.*, *14*, 1–43, doi:10.1016/0037-0738(75)90015-9.

Temmerman, S., P. Moonen, J. Schoelynck, G. Govers, and T.J. Bouma (2012), Impact of vegetation die-off on spatial flow patterns over a tidal marsh, *GRL*, *39*, 1–5, doi:10.1029/2011GL050502.

USGS (2010), ASTER Scene L1B_00305152004155804_2010120215.

Vermeer, M., and S. Rahmstorf (2009), Global sea level linked to global temperature., *Proc. Natl. Acad. Sci. U. S. A.*, *106*, 21527–21532, doi:10.1073/pnas.0907765106.

Wang, P., and M.H. Horwitz (2007), Erosional and depositional characteristics of regional overwash deposits caused by multiple hurricanes, *Sedimentology*, *54*, 545–564, doi:10.1111/j.1365-3091.2006.00848.x.

Weinstein, M.P., and D.A. Kreeger (2000), Concepts and Controversies in Tidal Marsh Ecology.

Wolinsky, M.A., and A.B. Murray (2009), A unifying framework for shoreline migration: 2. Application to wave-dominated coasts, *J. Geophys. Res.*, *114*, 1–13, doi:10.1029/2007JF000856.

Wolner, C.W. V, L.J. Moore, D.R. Young, S.T. Brantley, S.N. Bissett, and R.A. Mcbride (2013), Ecomorphodynamic feedbacks and barrier island response to disturbance : Insights from the Virginia Barrier Islands , Mid-Atlantic Bight , USA, *Geomorphology*, 1–14, doi:10.1016/j.geomorph.2013.03.035.

Xie, Y., Z. Sha, and M. Yu (2008), Remote sensing imagery in vegetation mapping: a review, *J. Plant Ecol.*, *1*, 9–23, doi:10.1093/jpe/rtm005.

Zhang, K., and S. Leatherman (2011), Barrier Island Population along the U.S. Atlantic and Gulf Coasts, *J. Coast. Res.*, 356–363, doi:10.2112/JCOASTRES-D-10-00126.1.

Zhang, K., B. Douglas, and S. Leatherman (2004), Global warming and coastal erosion, *Clim. Change*, 41–58, doi:10.1023/B:CLIM.0000024690.32682.48.

Tables and Figures

Table 1. Index parameters for stratigraphic units used in *GEOMBEST+* experiments.

	Parameter	Range of Values Tested				Source Used
		Barrier	Bay	Marsh	Underlying	
Marsh-width experiments	Sand content	1	0.5	0.1	0.75	*Brenner* [2012] PSA analysis of marsh sediment
	Erodibility	1	1	0.01-1	1	*Brenner* [2012]
	Organic content (O_C)	0	0	0.5	0	LOI Experiments *Weinstein and Kreeger* [2000]
Island-migration experiments	Bay sediment flux (Q_B)	2 - 20 m^3/m/yr, in increments of 2				*Schwimmer* [2001]
	Relative sea level rise rate (R)	1 - 10 mm/yr, in increments of 1				*IPCC* [2014]
	Overwash volume flux (Q_{OW})	0.2 - 2.0 m^3/m/yr, in increments of 0.2				*Fisher et al.* [1974] *Leatherman and Zaremba* [1987]
	Maximum bay erosion rate (E_{max})	10 cm/yr				Determined empirically from model simulations
	Resuspension depth (D_R)	0.4 m				

Table 2. Q_{OW} and Q_B parameter values used to set marsh width for long-term island-migration experiments, and resulting island migration rates.

Backbarrier Sediment Content	Parameters		Marsh Width		Island Migration Rate (m/yr)
	Q_{OW} (m^3/m/yr)	Q_B (m^3/m/yr)	Average (m)	Alternate state	
Muddy	0.5	5	0	Empty basin	1.8
Mixed	1	5	0		1.8
Sandy	2	5	0		1.9
Muddy	0.5	8.5	129	Narrow marsh	1.3
Mixed	1	7.5	158		1.4
Sandy	2	7	171		1.4
Muddy	0.5	16	4279	Marsh-filled basin	1.2
Mixed	1	16	4224		1.3
Sandy	2	16	4157		1.4

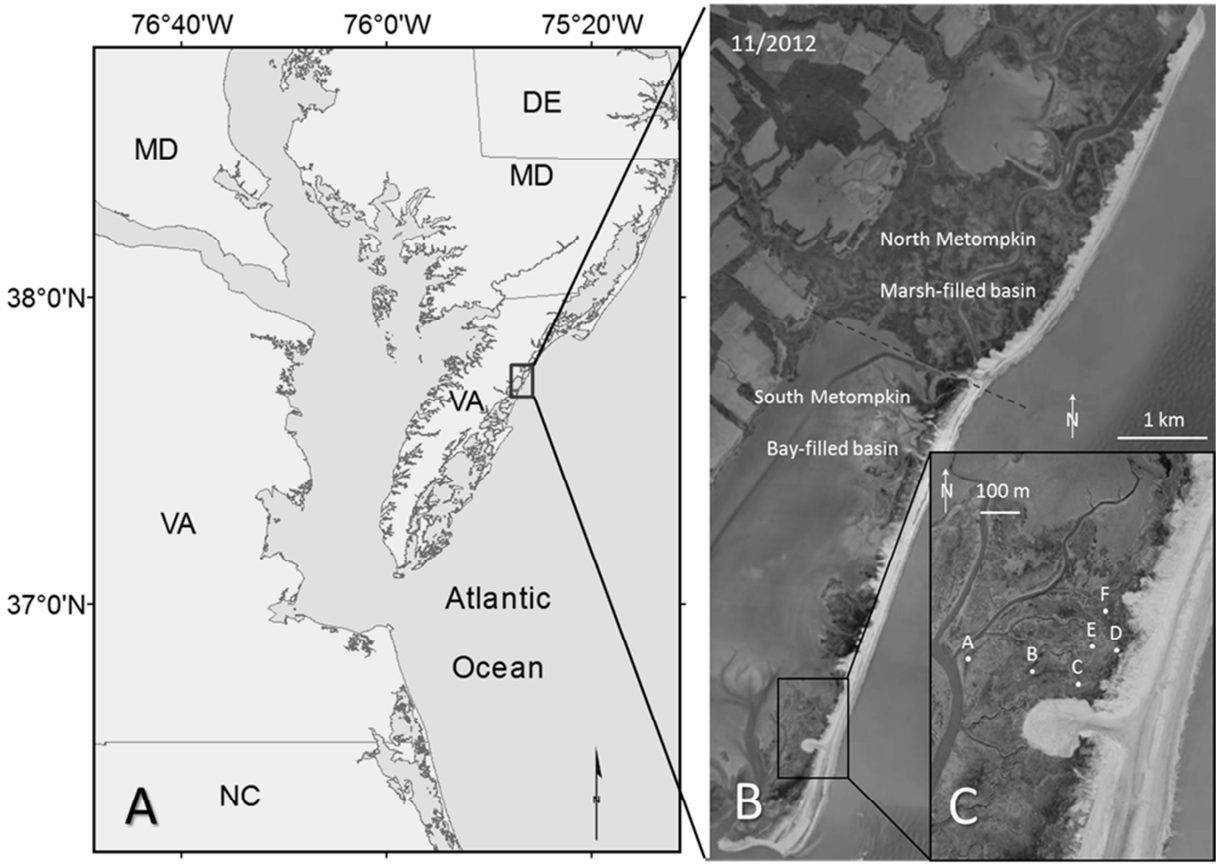

Figure 1. (A) Site location map of the Virginia Barrier Islands, located on the southern tip of the Delmarva Peninnsula. The location of Metompkin Island is shown in the gray box. (B) Aerial photograph of Metompkin Island showing variable backbarrier environments (Google Earth, TerraMetrics 2013). (C) Location of field sampling sites in the backbarrier marsh of Metompkin.

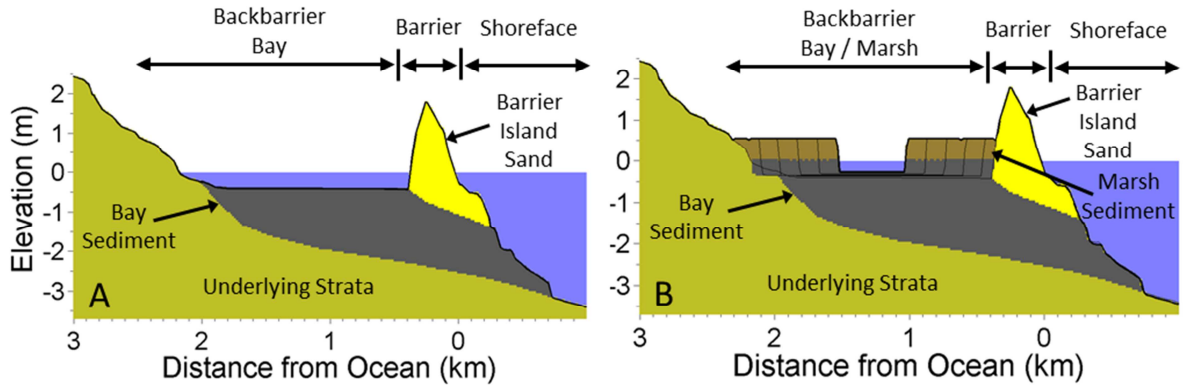

Figure 2. (A) Cross-shore profile of coastal morphology for a low-gradient barrier island coast, which serves as the initial condition for model experiments. GEOMBEST's three functional realms (shoreface, barrier, and backbarrier bay) and distinct stratigraphic units (barrier island sand, bay sediment, and underlying strata) comprise this example of a coastal tract. (B) *GEOMBEST+* output showing a coastal profile resulting from a bay sediment flux of 20 m^3/m/yr and a *R* of 0 mm/yr, , according to the three functional realms (shoreface, barrier, bay/marsh) and distinct stratigraphic units (barrier island sand, marsh sediment, bay mud, and underlying strata), which may erodein the new model, as in GEOMBEST. Ghost traces of marsh boundaries are plotted every 10 years.

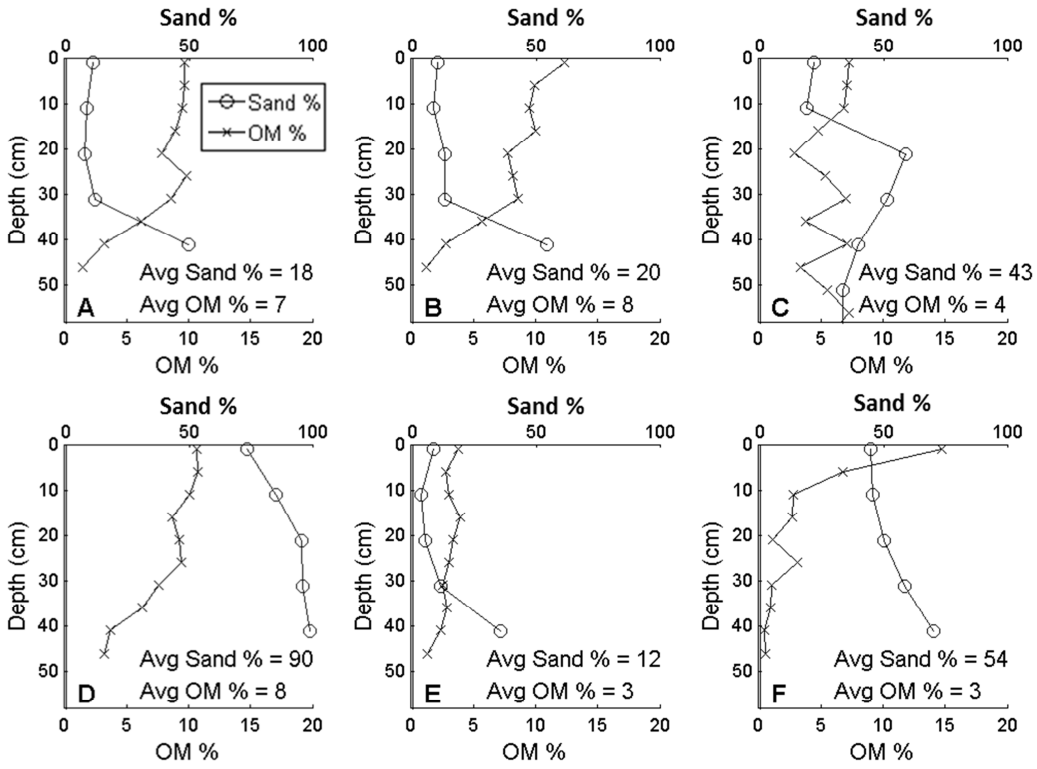

Figure 3. Plot of depth vs. sediment percent sand (top x-axis) and percent organic matter (bottom x-axis) for each of the six sampling sites A-F at the Metompkin Island backbarrier marsh (locations shown in Figure 1C).

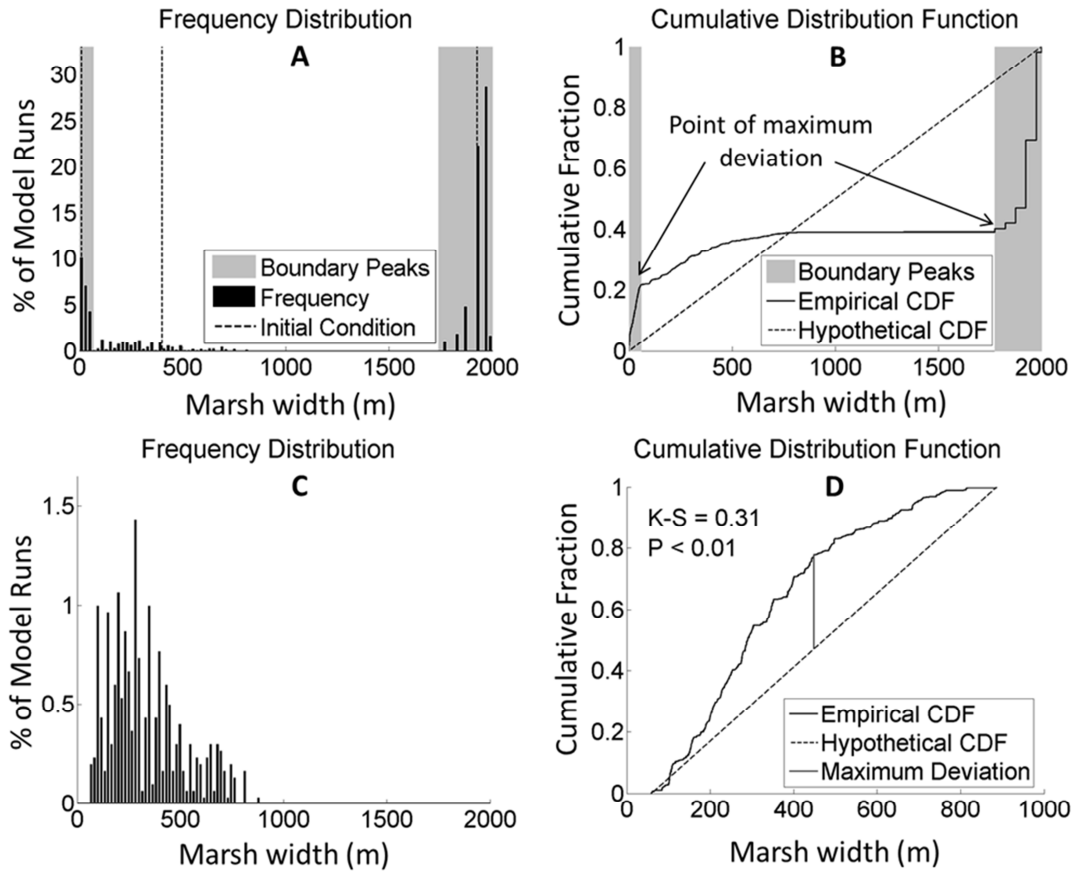

Figure 4. (A) Frequency distribution of backbarrier marsh width for the final time step from marsh-width experiments. Dashed lines indicate initial widths, and gray bars indicate the range of empty and filled basin peaks. (B) Gray bars indicate the range of widths within which peaks in frequency occur that are associated with marsh-filled basins (> 1775 m) and empty basins (< 67 m) based on the point at which the maximum deviation of the cumulative distribution function from the standard uniform distribution occurs. (C) Frequency distribution for those intermediate widths between the two boundary conditions. (D) Cumulative distribution of the intermediate widths, showing the maximum deviation from a random uniform distribution at 448 m, which is statistically significant at a 99% confidence level according to the Kolmogorov–Smirnov test.

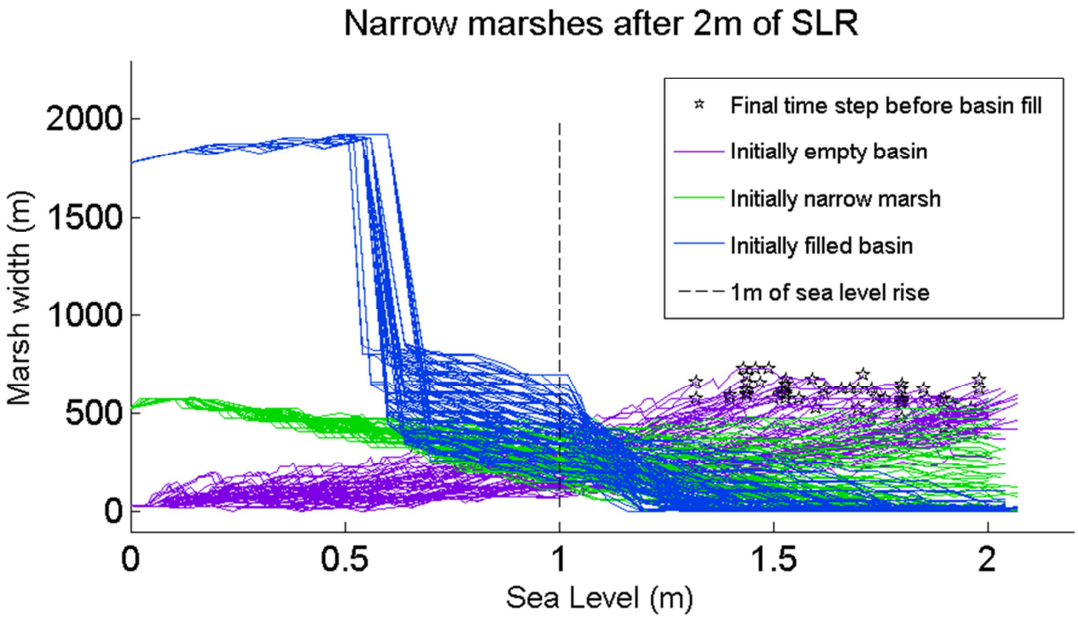

Figure 5. Change in marsh width as sea level rises for the 340 marshes (out of 3,000 simulations) that fell within the narrow marsh width range (150-450 m) after one meter of sea level rise in previous simulations. Each line represents a single simulation, color coded for initial position. The dashed line indicates marsh width after one meter of sea level rise. For simulations that are initially filled, marsh width drops rapidly once bays begin forming in the middle of the basin, causing a halving in the backbarrier marsh width. For simulations in which basins become marsh-filled, the last marsh width plotted comes from the final time step before the basin fills (plotted as a star). Approximately 90% of these runs reach either the empty or filled basin state after 2m of sea level rise.

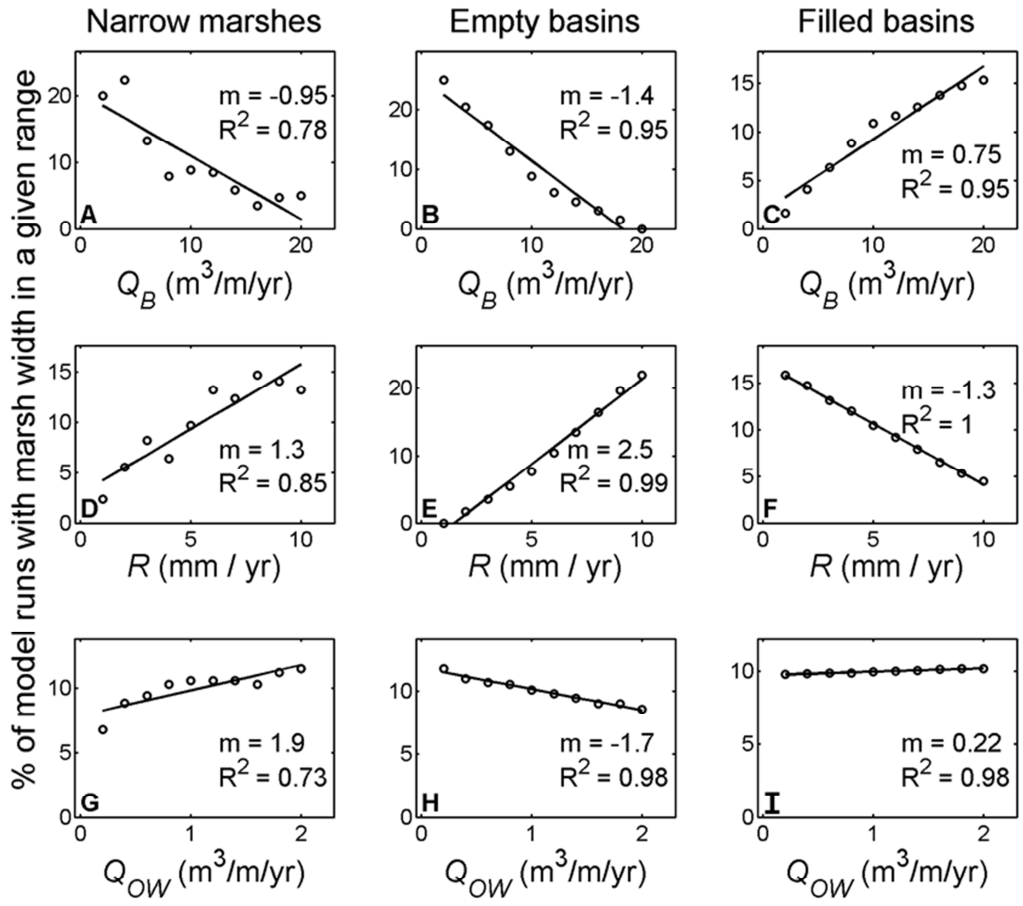

Figure 6. The relationships of Q_B (A-C), R (D-F), and Q_{OW} (G-I), to marsh width, broken down by the percent of runs that resulted in a marsh width within a given range. The ranges are defined by each of the three identified alternate states: empty basin (width < 67 m; panels A, D, and G), narrow marsh (width = 150 – 450 m; panels B, E, and H), and marsh-filled basin (width > 1775 m; panels C, F, and I), from simulations of 1 m of total sea level rise.

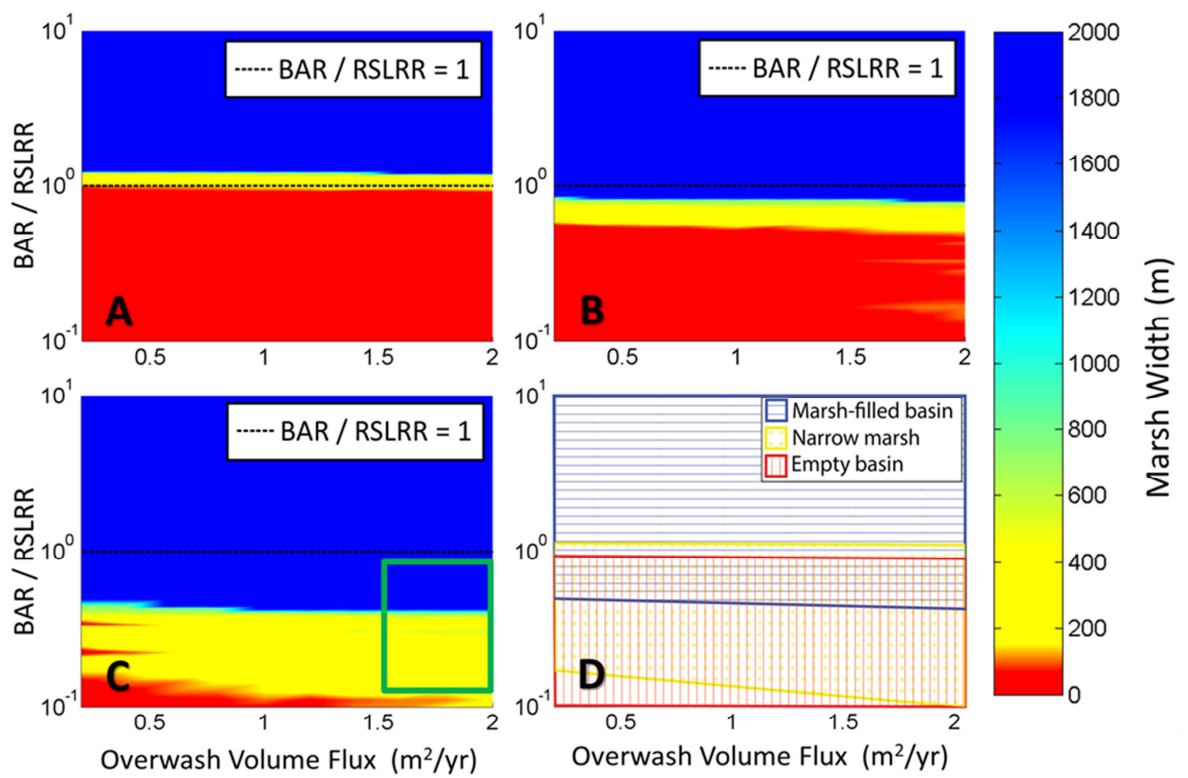

Figure 7. Phase diagram showing how marsh width changes within the range of parameter space for the initial condition of an empty basin (A), a narrow marsh (B) and a marsh-filled basin (C). BAR is the basin accretion rate, determined by dividing the Q_B by the width of the backbarrier basin. The dashed black line shows the position where bay accretion rate is equal to the relative sea level rise rate. The green box in the lower right-hand corner of panel C indicates where the VBIs lie within the parameter space. The extent of the phase space that is occupied by each identified alternate stable state is shown in D.

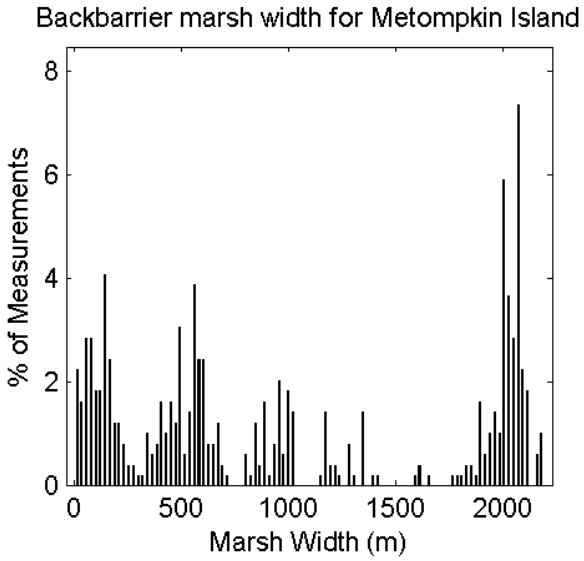

Figure 8. Frequency distribution of marsh widths for Metompkin Island, VA, as measured from ASTER satellite imagery.

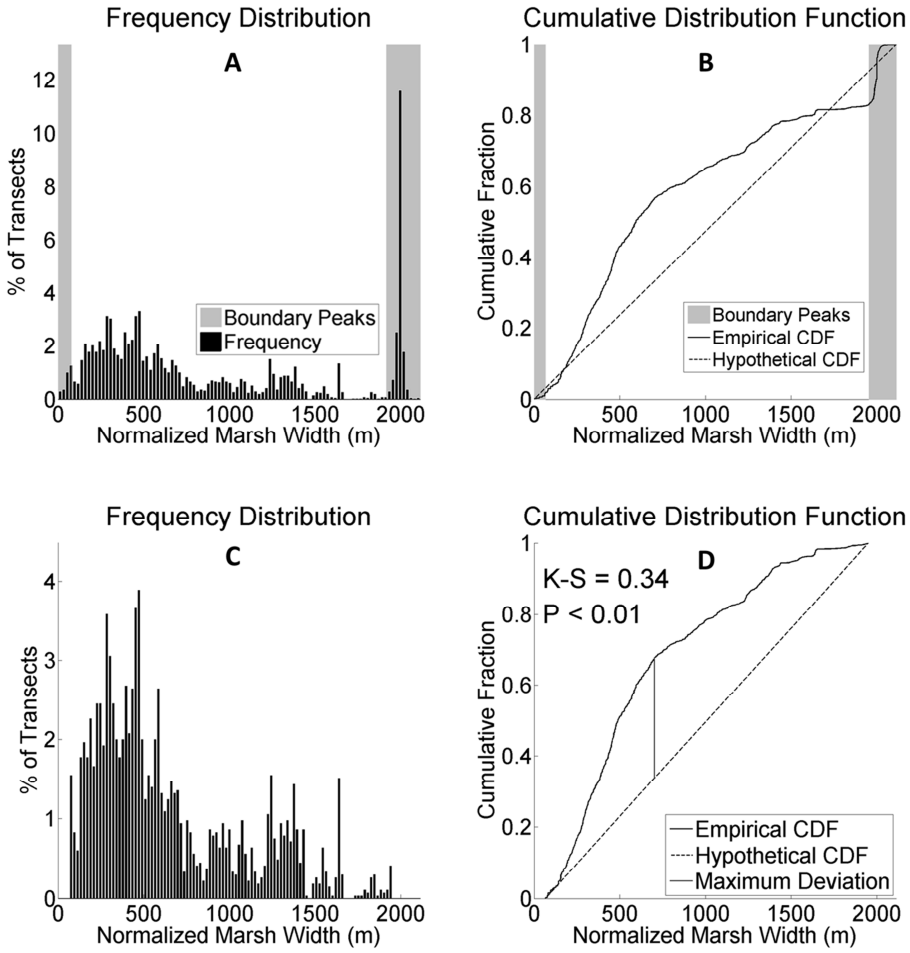

Figure 9. (A) Frequency distribution of backbarrier marsh width measurements from remote sensing observations of the entire VBIs. Measurements are normalized to a basin size of 2000 m by dividing the raw measurements of the backbarrier marsh width by the basin width, and multiplying by 2000 m. (B) Gray bars indicate the range of widths within which basins are completely filled with marsh (> 1950 m) based on the maximum deviation of the cumulative distribution function from the standard uniform distribution, or completely empty of marsh (< 67 m) based on the range derived from model experiments.. (C) Frequency distribution for the intermediate widths that are not associated with the boundary condition peaks. (D) Cumulative distribution function of the intermediate widths, showing that the maximum deviation from a standard uniform distribution occurs at 702 m. This deviation of the cumulative distribution function from the hypothetical distribution over widths from 150 m-700 m is statistically significant (99% confidence level) according to the Kolmogorov–Smirnov test.

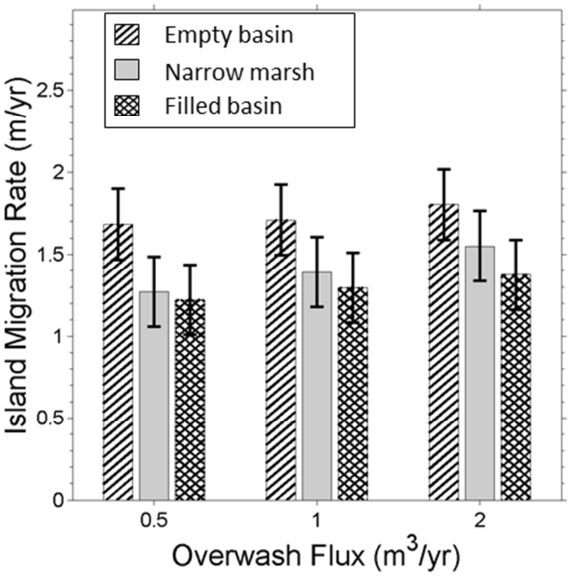

Figure 10. Plot of shoreline migration rate for 1000-yr simulation with a 4 mm/yr *R* and different backbarrier environments (Empty basin to marsh-filled basin; muddy to sandy). Error bars show one standard deviation from the mean.

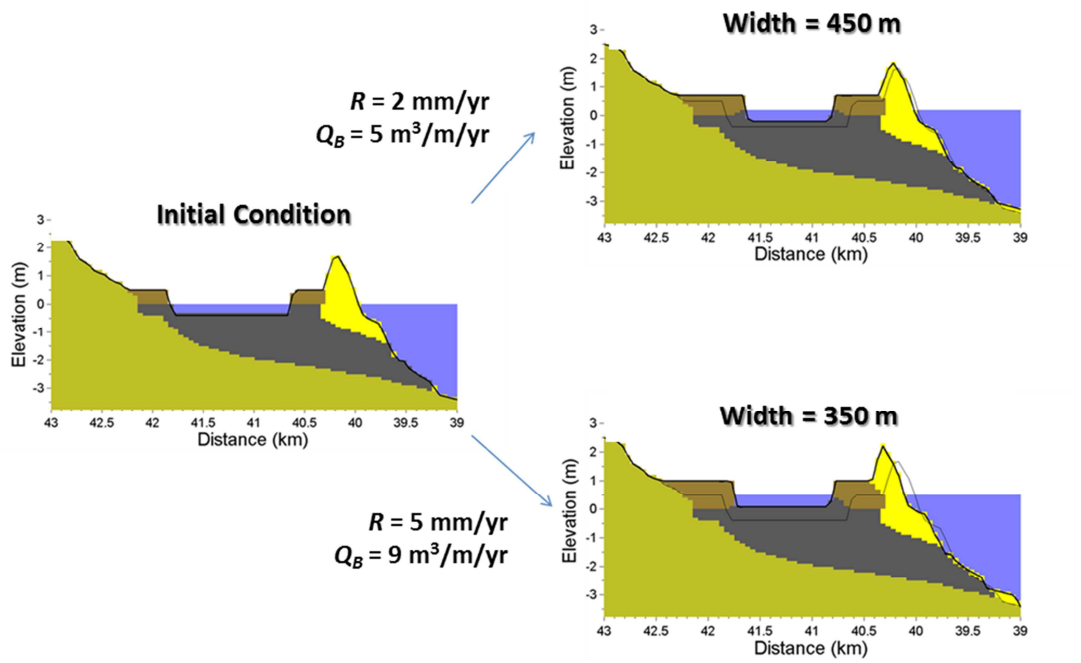

Figure 11. These plots show two 100-yr simulations arising from the same initial condition, but having varied parameter inputs such that they resulted in the same marsh progradation rate of 1.5 m/yr, but different final marsh widths, because of differences in the rate of island migration.